



Published in final edited form as:

*Soft Matter*. 2013 January 7; 9(1): 82–89. doi:10.1039/C2SM26996A.

## pH-triggered self-assembly of biocompatible histamine-functionalized triblock copolymers<sup>†</sup>

Pontus Lundberg<sup>a</sup>, Nathaniel A. Lynd<sup>a</sup>, Yuning Zhang<sup>b</sup>, Xianghui Zeng<sup>b</sup>, Daniel V. Krogstad<sup>a</sup>, Tim Paffen<sup>a</sup>, Michael Malkoch<sup>c</sup>, Andreas M. Nyström<sup>b</sup>, and Craig J. Hawker<sup>a,d</sup>

<sup>a</sup>Materials Research Laboratory, University of California, Santa Barbara, CA 93106, USA

<sup>b</sup>Swedish Medical Nanoscience Center, Department of Neuroscience, Karolinska Institutet, Retzius väg 8, Stockholm SE-171 77, Sweden

<sup>c</sup>Department of Fibre and Polymer Technology, KTH Royal Institute of Technology, School of Chemical Science and Engineering, Teknikringen 56-58, Stockholm SE-100 44, Sweden

<sup>d</sup>Department of Chemistry and Biochemistry and Materials Department, University of California, Santa Barbara, CA 93106, USA

### Abstract

Histamine functionalized poly(allyl glycidyl ether)-*b*-poly(ethylene glycol)-*b*-poly(allyl glycidyl ether) (PAGE-PEO-PAGE) triblock copolymers represent a new class of physically cross-linked, pH-responsive hydrogels with significant potential for biomedical applications. These telechelic triblock copolymers exhibited abrupt and reversible hydrogelation above pH 7.0 due to a hydrophilic/hydrophobic transition of the histamine units to form a network of hydrophobic domains bridged by a hydrophilic PEO matrix. These hydrophobic domains displayed improved ordering upon increasing pH and self-assembled into a body centered cubic lattice at pH 8.0, while at lower concentrations formed well-defined micelles. Significantly, all materials were found to be non-toxic when evaluated on three different cell lines and suggests a range of medical and biomedical applications.

### Introduction

Hydrogels have become an increasingly important class of materials for biomedicine, pharmaceuticals, coatings and cosmetics.<sup>1, 2</sup> Their utility is derived from their high water-content, yet solid-like mechanical properties derived from the presence of a three-dimensional network. The network can be formed by either covalent bonds or through physical interactions such as hydrophobic, electrostatic or hydrogen bonding.<sup>1–4</sup>

For many applications, it is desirable to have gels that respond to external stimuli, i.e. smart gels.<sup>5</sup> Smart gels can be tailored to be responsive to a change in the surrounding environment, such as temperature, pH, ionic strength, or light.<sup>2, 5–9</sup> Of these external

<sup>†</sup>Electronic Supplementary Information (ESI) available: Additional characterization of the material, gels and micelles including FT-IR, Raman, potentiometric titrations, rheology, DLS and CMC measurements can be found in the ESI. See DOI: 10.1039/b000000x/

stimuli, pH-responsive gels are of particular interest for biomedical applications since different intra- and extracellular compartments maintain varying levels of acidity or alkalinity. A highly relevant example is the difference in pH between healthy tissue and tumor tissue. In blood and extracellular fluids of healthy tissue the pH is 7.4, whereas intracellular components such as endosomes and lysosomes have lower pH.<sup>10</sup> Similarly, the pH of extracellular fluids in tumor tissues is lower, ca. 6.0, due to the elevated levels of metabolic byproducts such as lactic acid produced by cancer cells.<sup>11, 12</sup> For biomedical applications, such as in chemotherapeutic drug delivery, it is desirable to exploit these differences in pH by tailoring materials that respond dramatically and specifically within a narrow physiologically relevant pH range, e.g., pH 6.0 to 7.4.

Due to the potential of polymer-based therapeutics that exploit these differences in pH, an extensive amount of effort has been directed toward developing pH-responsive materials. In one example, Thomas *et al.* prepared copolymers of 2-ethylacrylic acid and methyl methacrylate which allowed the  $pK_a$  to be systematically increased to 6.5, compared to 5.7 for pure poly(2-ethylacrylic acid).<sup>13</sup> Philippova *et al.* used a similar strategy to tune the swelling of hydrogels by copolymerizing acrylic acid, *N,N'*-methylenebis(acrylamide), and *n*-alkyl acrylates,<sup>14</sup> while single component systems like 2-(diisopropylamino)ethyl methacrylate (DPA), which has a  $pK_a$  between 6 and 7, have also been developed.<sup>15, 16</sup> However, a major drawback to many of these systems is toxicity, for example the DPA-based polymer can release 2-(diisopropylamino)ethanol upon hydrolytic degradation which is highly toxic.<sup>17</sup> Looking to nature for inspiration, researchers have addressed this toxicity issue by using natural, non-toxic building blocks. Our attention was therefore directed to developing materials based on the amino acid histidine and its derivative histamine, which are both non-toxic and have ideal  $pK_a$ 's of ca. 6.5.<sup>18</sup> At neutral or basic pH, e.g. in blood, the imidazole group is uncharged and hydrophobic; whereas in acidic environments, such as in the endosome or extracellular sites of tumors, the imidazole is charged and hydrophilic. As an example, poly(histidine)-*b*-poly(ethylene oxide) was shown to exhibit pH-dependent micellization, and promote endosomal escape of the carrier system to achieve higher efficiency in delivering chemotherapeutic drugs, such as paclitaxel.<sup>18, 19</sup>

While covalently crosslinked hydrogels have been widely used in various coating applications, the need for degradation and versatile in- and ex-situ processing has focused attention on the development of physically crosslinked hydrogels. As an effective and versatile strategy for the preparation of bio-compatible hydrogels it was decided to combine histidine-based building blocks with the self-assembly of telechelic ABA-type triblock-copolymers where the mid-block (B) is hydrophilic and physical association between the outer blocks (A) forms physical cross-links.<sup>20</sup> Our group has recently developed a modular approach to the synthesis of ionic hydrogels based on poly(allyl glycidyl ether)-*b*-poly(ethylene oxide)-*b*-poly(allyl glycidyl ether) (PAGE-PEO-PAGE). The key step in this strategy is functionalization of the allyl groups using thiol-ene chemistry,<sup>3</sup> which has proven to be an extremely versatile and effective method for polymer functionalization.<sup>21–25</sup> In this study, a histamine-functional thiol was synthesized and reacted onto a PAGE-PEO-PAGE triblock-copolymer through thiol-ene chemistry and the structure/properties of the resulting hydrogels investigated for a range of polymer concentrations and pH values (Figure 1). At

polymer concentrations of 10 wt%, small angle x-ray scattering (SAXS) and rheometry were used to investigate the pH-dependent gel formation. At lower concentrations, the triblock copolymers formed pH-responsive micelles which were investigated using cryo-TEM and DLS.

## Experimental

### Materials

The synthesis of PAGE-*b*-PEO-*b*-PAGE with 26 wt% PAGE at a molecular weight of 27 kg/mol (PAGE<sub>3.5k</sub>-*b*-PEO<sub>20k</sub>-*b*-PAGE<sub>3.5k</sub>) has been reported previously.<sup>3</sup> Histamine (97.0%),  $\gamma$ -thiobutyrolactone (98%), 2,2-dimethoxy-2-phenylacetophenone (99%) (DMPA), bromothymol blue (BTB) solution in ethanol, pyrene (p.a.), 3-(4,5-dimethylthiazol-2-yl)-2,5-diphenyl tetra sodium bromide (MTT), and Dulbecco's modified Eagle's medium (DMEM) were purchased from Sigma–Aldrich and used without further purification. Acetonitrile (HPLC) and methanol (ACS) were purchased from Fisher Scientific. Dialysis membranes with MWCO 3500 Da were purchased from Spectrum labs. 100 mM buffer solutions were prepared by mixing NaH<sub>2</sub>PO<sub>4</sub>·H<sub>2</sub>O (ACS, EMD chemicals) and Na<sub>2</sub>HPO<sub>4</sub>·7H<sub>2</sub>O (ACS, EMD chemicals) with deionized water in appropriate amounts to reach the targeted pH. Fetal bovine serum (FBS) and penicillin/streptomycin solution were obtained from Hyclone Laboratories. MDA-MB-231, and MCF-7 cells were purchased from the American Type Culture Collection (ATCC). RAW 264.7 (Mouse leukemic monocyte macrophage cell line, originating from ATCC) was obtained from the laboratory of Prof Richter-Dahlfors at the Swedish Medical Nanoscience Center, Department of Neuroscience Karolinska Institutet, Stockholm Sweden.

### Instrumentation

Rheological experiments were performed on a Rheometrics Scientific ARES II rheometer with parallel-plate geometry (25mm or 50 mm diameter). Frequency sweeps were performed using 2% strain for gel-like materials and 6 % for liquid-like materials. Strain sweeps were performed at a frequency of 1 Hz and all frequency sweeps were performed within the linear viscoelastic regime. All experiments were performed at room temperature (21–24 °C).

Small angle x-ray scattering (SAXS) was performed at beamline DND-CAT line 5 at the Advanced Photon Source, Argonne National Laboratory. The samples were packed into 1 mm diameter quartz capillaries through the use of a centrifuge. The samples were then flame sealed and the top was covered with epoxy in order to prevent drying.

Dynamic light scattering experiments were performed on a DynaPro NanoStar from Wyatt. Reported values are average values of 20 acquisitions.

Fluorescence spectroscopy was performed on Cary Eclipse from Varian using an excitation wavelength of 332 nm and emission spectra were collected between 350–420 nm.

Samples for cryogenic transmission electron microscopy (cryo-TEM) were prepared at a polymer concentration of 1 mg/mL. The samples were then vitrified using the environmentally controlled FEI Mark IV Vitrobot (24°C, 100% humidity). A 3.5 $\mu$ L droplet

was placed on a glow discharged copper grid coated with a lacey Formvar support film. The samples were blotted once before being plunged into liquid nitrogen cooled liquid ethane. The samples were placed in a Gatan cryoholder and were kept below  $-170^{\circ}\text{C}$  throughout imaging. The samples were imaged at 200kV with an FEI T20 TEM using low dose imaging mode. Images were recorded digitally using a Gatan Ultrascan 1000 CCD camera and analyzed using Gatan Digital Micrograph and ImageJ software. Using the ellipse tool in ImageJ, the size of 100 particles in each picture was measured and recorded.

## Methods

### Synthesis of N-(2-(1H-imidazol-4-yl)ethyl)-4-mercaptobutanamide (Hist-SH)

In a 250 ml round bottom flask equipped with a Teflon-coated stir bar and a condenser, 10.1 g (99.0 mmol) of  $\gamma$ -thiobutyrolactone, 10.0 g (90.0 mmol) of histamine and 150 ml of acetonitrile was added. The reaction mixture was heated to  $95^{\circ}\text{C}$  using an oil bath and the reaction was allowed to proceed overnight. The reaction was cooled to room temperature and the product was isolated by filtration and dried under vacuum yielding a pale yellow solid. Yield 18.3 g (95%).  $^1\text{H-NMR}$   $\delta$  (ppm) = 1.87 (p, 2H,  $J = 30$  Hz,  $-\text{CH}_2-\text{CH}_2-\text{CH}_2-$ ), 2.30 (t, 2H,  $J = 15$  Hz,  $-\text{C}(=\text{O})-\text{CH}_2-$ ), 2.49 (t, 2H,  $J = 10$  Hz,  $-\text{CH}_2-\text{SH}$ ), 2.79 (t, 2H,  $J = 15$  Hz, imidazole- $\text{CH}_2-$ ), 3.44 (t, 2H,  $J = 15$  Hz,  $-\text{CH}_2-\text{NH}-\text{C}(=\text{O})-$ ), 6.86 (s, 1H,  $-\text{NH}-\text{CH}=\text{C}<$ ), 7.60 (s, 1H,  $-\text{NH}-\text{CH}=\text{N}-$ ).  $^{13}\text{C-NMR}$   $\delta$  = 23.06, 26.39, 29.89, 34.11, 38.90, 134.65, 173.94. FT-IR  $\nu$  ( $\text{cm}^{-1}$ ) = 3230, 3130, 2980, 2895, 1640, 1575, 1495, 1420, 1360, 1300, 1253, 1225, 1195, 1090, 1060, 929, 889, 833, 736, and 714. Mass spectrometry ESI/TOF found 236.0811 Da [ $\text{M}+\text{Na}^+$ ], calculated 236.0834 Da [ $\text{M}+\text{Na}^+$ ].

### Synthesis of histamine functional triblock-copolymer (PHGE-b-PEO-b-PHGE)

In a 250 ml round bottom flask equipped with a Teflon-coated stir bar, 5.0 g (0.19 mmol) of **PAGE<sub>3.5k</sub>-b-PEO<sub>20k</sub>-b-PAGE<sub>3.5k</sub>**, 4.7 g (22.2 mmol) of **Hist-SH** and 125 ml of MeOH was added. Once all of the reactants were dissolved, 0.14 g (0.56 mmol) of DMPA was added and the solution sparged with Ar (g) for five minutes. The solution was then irradiated with 365 nm light for 90 minutes under stirring and subsequently transferred to a dialysis bag with a MWCO of 3500 Da. After dialysis in  $4 \times 3.5$  L of MeOH, the purified material was isolated by evaporation and dried under vacuum overnight to afford a tacky, yellow solid. Yield 6.7 g (91%)  $^1\text{H-NMR}$   $\delta$  = 1.85 (m,  $-\text{S}-\text{CH}_2-\text{CH}_2-\text{CH}_2-\text{O}-$  and  $-\text{C}(=\text{O})-\text{CH}_2-\text{CH}_2-\text{CH}_2-\text{S}-$ ), 2.31 (t,  $J = 15$  Hz,  $-\text{C}(=\text{O})-\text{CH}_2-$ ), 2.52 (t,  $J = 15$  Hz,  $-\text{C}(=\text{O})-\text{CH}_2-\text{CH}_2-\text{CH}_2-\text{S}-$ ), 2.60 (t,  $J = 15$  Hz  $-\text{S}-\text{CH}_2-\text{CH}_2-\text{CH}_2-\text{O}-$ ), 2.79 (t,  $J = 15$  Hz, imidazole- $\text{CH}_2-$ ), 3.44 (t,  $J = 15$  Hz,  $-\text{CH}_2-\text{NH}-\text{C}(=\text{O})-$ ), 3.49–3.71 (m, backbone), 6.86 (s,  $-\text{NH}-\text{CH}=\text{C}<$ ), 7.61 (s,  $-\text{NH}-\text{CH}=\text{N}-$ ).  $^{13}\text{C-NMR}$   $\delta$  = 28.44, 29.240, 30.77, 32.28, 33.58, 41.696, 72.30, 72.54, 72.70, 72.86, 73.02, 73.84, 81.46, 119.25, 137.43, 176.51. FT-IR  $\nu$  ( $\text{cm}^{-1}$ ) = 3418, 3275, 3121, 2880, 2695, 2659, 1644, 1554, 1466, 1454, 1359, 1342, 1279, 1241, 1145, 1100, 1060, 962, 841, 755, 707, 663. FT-Raman  $\nu$  ( $\text{cm}^{-1}$ ) = 3110, 2912, 2885, 1644, 1567, 1478, 1442, 1363, 1281, 1235, 1142, 1060, 1029, 844, 649, 364, 278.

### Potentiometric titrations

60 mg of polymer was added to 50 ml of DI water and the pH was adjusted to 2.0 using 1 M HCl. Once all the **PHGE-b-PEO-b-PHGE** had dissolved and the pH was stable, 1 M NaOH

was added in 20  $\mu\text{l}$  portions, the pH was allowed to stabilize and the pH was recorded. Once the pH had reached 12.0 the titration was reversed by adding 1 M HCl in 20  $\mu\text{l}$  portions while measuring the pH until the pH had returned to 2. This procedure was then repeated two more times. As a reference, a NaCl solution containing 60 mg of NaCl in 50 ml of DI water was used.

### Preparation of gels

In a 20 ml vial with a screw cap, 400 mg of **PHGE-*b*-PEO-*b*-PHGE** was dissolved in 400  $\mu\text{l}$  of 0.1 M HCl followed by the addition of 3.2 ml of 100 mM phosphate buffer solution. After mixing for a short time using a vortexer, the gel was allowed to equilibrate for 2 days before the gels were characterized.

### Preparation of micelles

In a 20 ml vial equipped with a stir bar and a screw cap, 10 mg of **PHGE-*b*-PEO-*b*-PHGE** and 10 ml of phosphate buffer solution (filtered through a 0.45  $\mu\text{m}$  nylon syringe filter) was added. After stirring vigorously for 6 h, the solution was allowed to stand overnight without stirring. The micelles were subsequently characterized using DLS and cryo-TEM. The critical micelle concentration (CMC) was determined by a fluorescent probe technique using pyrene.<sup>26</sup>

### Toxicology – MTT assay

Human breast cell lines MDA-MB-231, and MCF-7 and mouse monocyte macrophage cell line RAW 264.7 were cultured in DMEM (pH7.4) supplemented with 10% FBS and 1% penicillin/streptomycin solution at 37°C in a humidified atmosphere with 5% CO<sub>2</sub>. The breast cancer cells were harvested enzymatically by trypsinization while RAW 264.7 was mechanically harvested by scraping. Three different cells lines were separately seeded into 96-well plates at a density of  $5 \times 10^4$  cells per well in 100  $\mu\text{L}$  DMEM (pH 7.4) and cultured for 24 h. The medium in each well was then replaced by 100  $\mu\text{L}$  of fresh medium (pH 6.7, 7.0 or pH 7.4) containing various concentrations of the triblock copolymer. The cells were incubated for another 48 h or 72 h, followed by the addition of 10  $\mu\text{L}$  MTT solution (5 mg/mL) to each well. After the cells were incubated for an additional 4 h, 100  $\mu\text{l}$  SDS solutions (10%) was added to each well. The absorbance was measured after 18 h in a plate reader at 570 nm.

## Results and Discussion

The imidazole group of histidine is of specific interest as a pH-responsive unit due to its biocompatibility as well as the physiologically relevant pH range (6.0–7.4) for protonation. For attachment to our previously-developed alkene functionalized polyether platform, a thiol-functional imidazole was initially targeted in tandem with orthogonal thiol-ene chemistry. In developing this synthesis strategy, we were inspired by the well-known reaction between amines and homocysteine, which has been used in small molecule chemistry<sup>27</sup> as well as for protein modification<sup>28</sup>. Hence, histamine and  $\gamma$ -thiobutyrolactone were chosen as the starting materials and reacted by simply mixing the two compounds in acetonitrile and heating (Scheme 1). Upon mixing at room temperature, histamine remain insoluble;

however, once the temperature reaches 95 °C, the histamine dissolves and product formation seen as precipitation of a yellow solid. After allowing the reaction to proceed overnight, it was cooled to ambient temperature and the product (**Hist-SH**) isolated by filtration (95%). Functionalization of the PAGE-PEO-PAGE triblock-copolymer was then achieved through photochemical, thiol-ene chemistry with quantitative conversion being achieved using 1.5 equivalents of thiol-functional histamine per allyl group (Scheme 1). After purification by dialysis in methanol, the functionalized triblock-copolymer (**PHGE-*b*-PEO-*b*-PHGE**) was isolated in 91% yield with <sup>1</sup>H-NMR spectroscopy showing the disappearance of peaks corresponding to the allyl group and appearance of unique resonances for the thio-histamine unit (peaks a', b', h', and g') (Figure 2). Removal of the excess histamine and degradation products from the initiator was monitored by <sup>1</sup>H-NMR, which also confirmed >95% of the histamine in the sample was attached to the polymer. Additionally, FT-IR and FT-Raman also confirmed the quantitative incorporation of histamine units (see Figure ESI1 and Figure ESI2). As expected, the functionalized **PHGE-*b*-PEO-*b*-PHGE** triblock copolymer was found to have poor solubility in most organic solvents and basic aqueous solutions; however, methanol and acidic aqueous solutions readily dissolved the product.

In order to characterize the pH-responsiveness of **PHGE-*b*-PEO-*b*-PHGE**, potentiometric titration was performed (Figure ESI3) In order to characterize the pH-responsiveness of **PHGE-*b*-PEO-*b*-PHGE**, potentiometric titration was performed (Figure ESI3) The ability to control gel formation with changes in pH was initially demonstrated through encapsulation of the pH-indicator, bromothymol blue (BTB). To a 20 wt% solution of **PHGE-*b*-PEO-*b*-PHGE** in 1 M HCl, was added BTB to give a yellow colored solution (indicating acidic pH), addition of 1 M NaOH then resulted in the instantaneous formation of a green/blue colored gel (indicating neutral pH). Cycling between a green/blue gel and yellow solution could then be achieved by simply adding acid or base with no change in physical properties after repeated cycling. These results suggest that the histamines indeed switch between its hydrophilic and a hydrophobic state as expected. To further explore gelation and the viscoelastic properties of these gels, a set of 10 wt% samples were prepared in buffer solutions from pH 8.0 to 5.0 and as can be seen in Figure 3, a distinct transition from a free-standing gel to liquids of decreasing viscosity is observed on changing pH. Of particular note is the sharp change in properties between pH values of 6.6 and 7.4, which is within the range of pH-differences that is expected when moving from healthy tissue to cancerous or inflammatory tissue in the human body.<sup>10-12</sup> The mechanical properties of these gels were then probed with a series of rheological experiments which revealed viscoelastic properties consistent with gels at pH 8.0 and pH 7.4 (Figure ESI4). For the pH 8.0 sample, a crossover is observed at 0.25 Hz corresponding to a relaxation time of 0.65 s, while for the pH 7.4 sample, this transition is observed at 1.9 Hz and leads to a relaxation time of 0.08 s.<sup>30</sup> Significantly, at pH 8, a *G'* of 1.1 kPa was observed for the 10 wt% **PHGE-*b*-PEO-*b*-PHGE** gel, which is comparable to previous reports on pH responsive ABA gelators and further demonstrates the utility of this structural platform (Figure 4).<sup>9, 16, 31</sup> Lowering the pH to 7.0 no crossover frequency can be observed and the material behaves as a viscous liquid. Additional decrease in pH results in further reduction of both *G'* and *G''*.

In order to characterize the pH-responsiveness of **PHGE-*b*-PEO-*b*-PHGE**, potentiometric titration was performed (Figure ESI3) and compared with a NaCl control solution. Significantly, a buffering region from pH 3 to 8 is observed and this buffering agrees well with other polymeric materials having an imidazole as the only pH-responsive moiety.<sup>19, 29</sup> Within the pH range of 3 to 8, the histamine units transition between a protonated hydrophilic state and a deprotonated hydrophobic state which is in agreement with the design of the triblock copolymer architecture of **PHGE-*b*-PEO-*b*-PHGE** and should result in pH-triggered self-assembly into gels or micelles.

Further analysis of the rheological properties reveal that the dynamic viscosity also drops as the pH is lowered (Figure ESI6) indicating that protonation of the imidazole groups reduces hydrophobic interactions and the resulting aggregate size. However, lowering the pH below 5.8 did not result in a further reduction in the viscosity. This suggests that although some imidazole units were still charge neutral, as supported by the titrations, there were too few to interact with each other in a significant manner. The relationship between gel formation and mesostructural differences underlying changes in viscoelasticity with pH was then examined by small angle X-ray scattering. Increasing the pH revealed several trends (Figure 5): the domain spacing increased from 20 nm at pH 6.6 to 26 nm at pH 8.0 with microphase-separation and long-range structural ordering increasing with pH.<sup>32</sup> From the  $q^*$  value of the gel at pH 8.0, the unit cell distance was calculated to be 37 nm ( $a=2^{3/2}\pi q^{*-1}$ ) based on a cubic lattice with BCC symmetry and the full reversibility associated with this assembly demonstrates the robustness of the histamine units as a structural directing unit.

The power of combining an amphiphilic triblock-copolymer architecture with the reversible association of the histamine units can also be appreciated through the formation of flower-like micelles at low concentration.<sup>33</sup> As demonstrated previously, polymer micelles based on triblock copolymers are of specific interest when compared to traditional diblock copolymer micelles for use in therapeutics<sup>34</sup> as they benefit from the enhanced permeability and retention effect (EPR) and increased biocompatibility.<sup>35</sup> In order to explore the micelle formation of **PHGE-*b*-PEO-*b*-PHGE**, low concentration (0.1 wt%) solutions were prepared at pH 5.0 to 8.0. Significantly, micelles were observed by DLS and cryo-TEM throughout the entire pH-range; however, their distribution differed greatly (see ESI7-12). At pH 8.0 and 7.4, narrow size distributions were observed (mean intensity radius of 40 nm and 34 nm respectively), whereas a broad range of particle sizes were observed at lower pH. This difference can also be clearly seen on analysis by cryo-TEM (Figure 6). Further investigation of the micelles was performed by determining the CMC at different pH values using a fluorescent probe technique (Figure ESI13) with the CMC (*ca.* 50  $\mu\text{g/ml}$ ) being independent of pH. These results suggest that micellization is not primarily driven by the change in protonation of the imidazole group, and instead, is driven by the permanent hydrophobic spacer between the backbone and the imidazole unit. A key design feature of these pH-responsive hydrogels for *in vivo* applications is the biocompatibility of the building blocks used in their construction. Toxicological evaluation was therefore performed by incubating the triblock copolymers with three different cell lines at three different pH values (6.7, 7.0 and 7.4) (Figure 7). Two well-known breast cancer cell lines MCF-7 and MDA-MB231, and one macrophage-like cell line RAW 264.7 were selected with the macrophages

being a good model for toxicity testing as they are an instrumental part of the innate immune system; clearing foreign bodies, such as nanoparticles from the blood stream, which may evoke an immune reaction.<sup>36</sup> The viability of cells was then evaluated using MTT staining after 48 and 72 h. Significantly, in the tested range of concentrations (0.01 µg/ml to 100 µg/ml), all cell lines displayed excellent viability indicating that the triblock copolymer assemblies have little or no toxicity over several orders of magnitude change in concentration. However, we can see a small reduction in the cell viability for the intermediate concentration of 1 µg/ml at pH 7, indicating perhaps that the self-assembly processes can have an effect on cell viability. Further understanding of effect requires a detailed investigation of the self-assembly process in complex media containing proteins.

## Conclusions

Among responsive hydrogels, pH-responsive gels are of particular interest as the human body displays significant variation in pH depending on tissue, intracellular compartment, and health status. Following a modular approach, a thiol- functional histamine unit (**Hist-SH**) with a pKa of ~6.5, which is ideally suited for *in-vivo* applications, was synthesized and used to functionalize **PAGE-*b*-PEO-*b*-PAGE**. The responsive nature of the triblock copolymer, **PHGE-*b*-PEO-*b*-PHGE**, allows free standing gels to be readily formed at pH >7 and at concentrations as low as 7 wt%. Interestingly, SAXS characterization of the 10 wt % gels showed that at pH 8.0, the hydrophobic domains order onto a BCC lattice while at low concentrations (0.1 wt%) micelles could be formed. The CMC of these micelles was independent of pH; however, the micellar size and size distribution was highly dependent on pH. Toxicological screening against three different cell lines showed that the material was non-toxic, which further supports the potential of *in vivo* use of the triblock material. These results suggest that the strategy of combining the responsiveness of histamine repeat units with the biocompatibility of functional polyethers may be of great utility for drug delivery applications with a passive targeting strategy and pH as an active trigger.

## Supplementary Material

Refer to Web version on PubMed Central for supplementary material.

## Acknowledgments

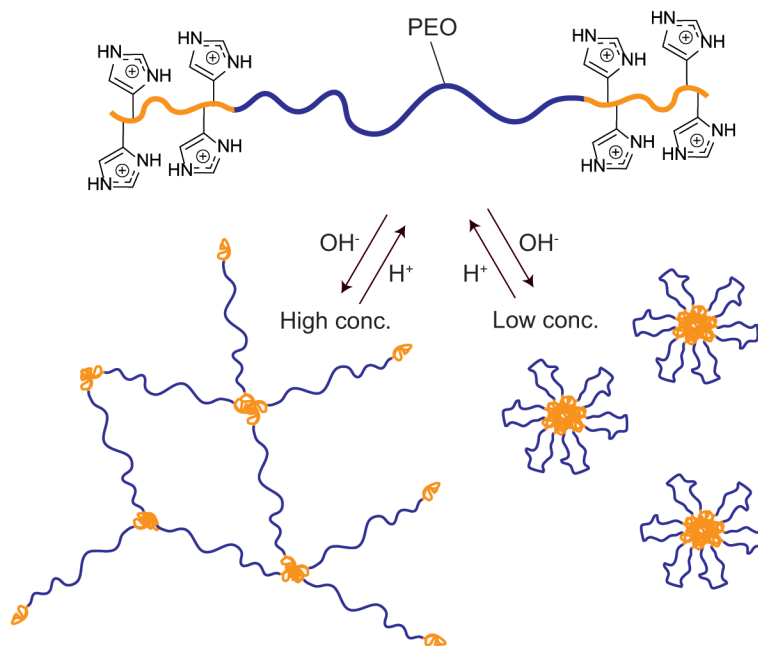
This work was partially supported by the National Institutes of Health as a Program of Excellence in Nanotechnology (HHSN268201000046C) (NAL and CJH) and the National Science Foundation through the MRSEC program (DMR-1121053 – PL, NAL, TP and CJH). PL would like to acknowledge the Wenner-Gren and Bengt Lundqvist foundations for financial support. AMN acknowledges financial support from STINT, Karolinska Institutet, Jeansson's Foundation, Åke Wibergs Foundation, Eva and Axel Wallströms Foundation, Percy Falks Foundation, Carl Bennet AB, The Swedish Research Council (VR) 2009-3259 (together with MM) and 2011-3720, The Swedish Medical Nanoscience Center and The Swedish Governmental Agency for Innovation Systems (Vinnova).

## Notes and references

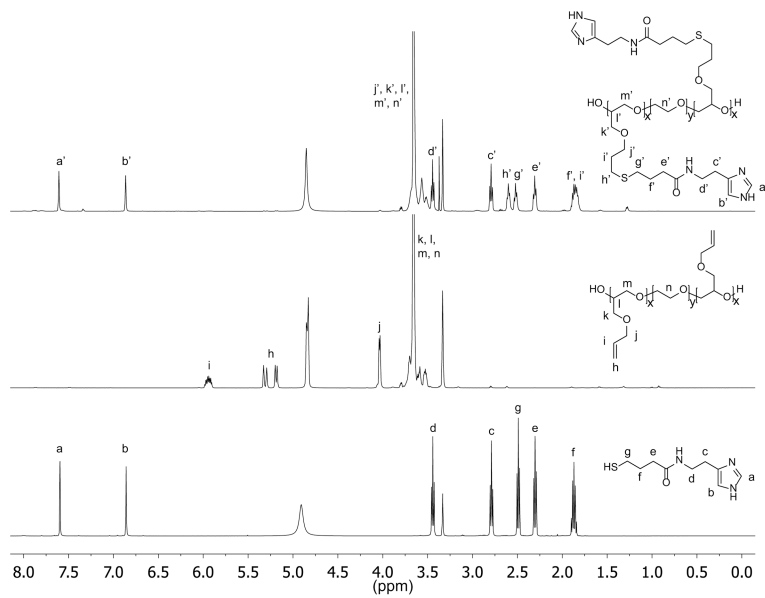
1. Ting Y, Long H, Malkoch M, Gamstedt EK, Berglund L, Hult A. J Polym Sci, Part A: Polym Chem. 2011; 49:4044–4054.
2. Peppas NA, Hilt JZ, Khademhosseini A, Langer R. Adv Mater. 2006; 18:1345–1360.



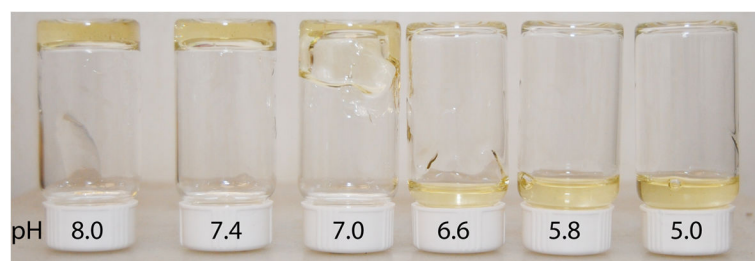
3. Hunt JN, Feldman KE, Lynd NA, Deek J, Campos LM, Spruell JM, Hernandez BM, Kramer EJ, Hawker CJ. *Adv Mater.* 2011; 23:2327–2331. [PubMed: 21491513]
4. Lemmers M, Sprakel J, Voets IK, van der Gucht J, Stuart MAC. *Angew Chem, Int Ed.* 2010; 49:708–711.
5. Zhu W, Nese A, Matyjaszewski K. *J Polym Sci, Part A: Polym Chem.* 2011; 49:1942–1952.
6. Ahn SK, Kasi RM, Kim SC, Sharma N, Zhou YX. *Soft Matter.* 2008; 4:1151–1157.
7. Qiu Y, Park K. *Adv Drug Delivery Rev.* 2001; 53:321–339.
8. Tsitsilianis C. *Soft Matter.* 2010; 6:2372–2388.
9. Madsen J, Armes SP. *Soft Matter.* 2012; 8:592–605.
10. Roos A, Boron WF. *Physiol Rev.* 1981; 61:296–434. [PubMed: 7012859]
11. Glynn SA, Albanes D. *Nutr Cancer.* 1994; 22:101–119. [PubMed: 14502840]
12. Tannock IF, Rotin D. *Cancer Res.* 1989; 49:4373–4384. [PubMed: 2545340]
13. Thomas JL, You H, Tirrell DA. *J Am Chem Soc.* 1995; 117:2949–2950.
14. Philippova OE, Hourdet D, Audebert R, Khokhlov AR. *Macromolecules.* 1997; 30:8278–8285.
15. Castelletto V, Hamley IW, Ma YH, Bories-Azeau X, Armes SP, Lewis AL. *Langmuir.* 2004; 20:4306–4309. [PubMed: 15969434]
16. Ma YH, Tang YQ, Billingham NC, Armes SP, Lewis AL. *Biomacromolecules.* 2003; 4:864–868. [PubMed: 12857066]
17. M. 2-(Diisopropylamino)ethanol; MSDS No. 471488 [Online]. Sigma-Aldrich; Saint Louis: Jan 19. 2012 <http://www.sigmaaldrich.com/catalog/product/aldrich/471488> [accessed Apr 27, 2012]
18. Park JS, Han TH, Lee KY, Han SS, Hwang JJ, Moon DH, Kim SY, Cho YW. *J Controlled Release.* 2006; 115:37–45.
19. Lee ES, Shin HJ, Na K, Bae YH. *J Controlled Release.* 2003; 90:363–374.
20. Kops J, Truelsen JH, Lei M, Armes SP. *Abstr Pap Am Chem Soc.* 2002; 224:U444–U444.
21. Lee BF, Kade MJ, Chute JA, Gupta N, Campos LM, Fredrickson GH, Kramer EJ, Lynd NA, Hawker CJ. *J Polym Sci, Part A: Polym Chem.* 2011; 49:4498–4504.
22. Kade MJ, Burke DJ, Hawker CJ. *J Polym Sci, Part A: Polym Chem.* 2010; 48:743–750.
23. Lowe AB. *Polym Chem.* 2010; 1:17–36.
24. Sumerlin BS, Vogt AP. *Macromolecules.* 2010; 43:1–13.
25. Iha RK, Wooley KL, Nystrom AM, Burke DJ, Kade MJ, Hawker CJ. *Chem Rev.* 2009; 109:5620–5686. [PubMed: 19905010]
26. Kalyanasundaram K, Thomas JK. *J Am Chem Soc.* 1977; 99:2039–2044.
27. Benesch R, Benesch RE. *Proc Natl Acad Sci U S A.* 1958; 44:848–853. [PubMed: 16590281]
28. Jakubowski, H.; Glowacki, R. *Advances in Clinical Chemistry.* Makowski, GS., editor. Vol. 55. Elsevier Academic Press Inc; San Diego: 2011. p. 81-103.
29. Ramirez SM, Layman JM, Bissel P, Long TE. *Macromolecules.* 2009; 42:8010–8012.
30. Nishinari, K. Vol. 136. Springer; Berlin/Heidelberg: 2009. p. 87-94.
31. Guvendiren M, Messersmith PB, Shull KR. *Biomacromolecules.* 2008; 9:122–128. [PubMed: 18047285]
32. Samples at pH 5.0 and 5.8 could unfortunately not be measured as the sample-tubes had broke during transport.
33. Hamley, IW. *The Physics of Block Copolymers.* Oxford University Press; Oxford: 1998.
34. Duncan R. *Nat Rev Drug Discov.* 2003; 2:347–360. [PubMed: 12750738]
35. Matsumura Y, Maeda H. *Cancer Res.* 1986; 46:6387–6392. [PubMed: 2946403]
36. Wu Z, Zeng X, Zhang Y, Feliu N, Lundberg P, Fadeel B, Malkoch M, Nystrom AM. *J Polym Sci, Part A: Polym Chem.* 2012; 50:217–226.



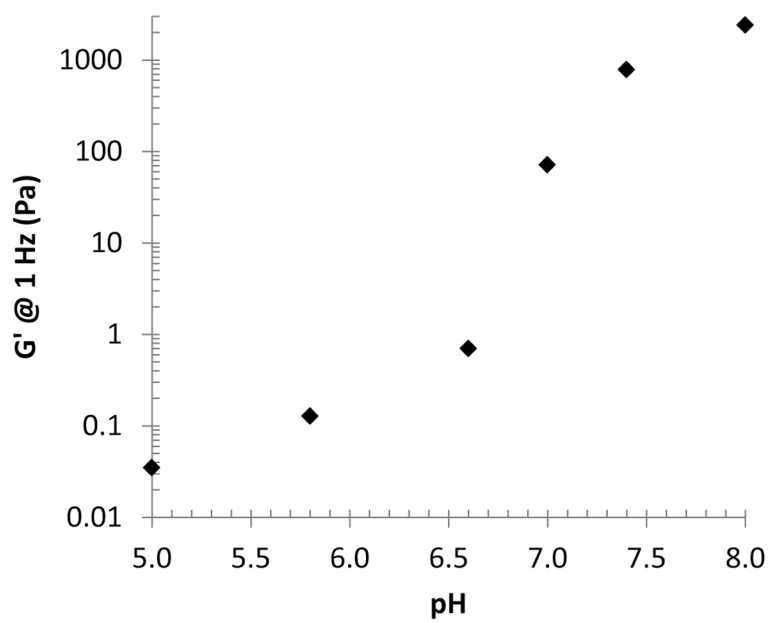
**Fig. 1.** Schematic strategy of the pH-responsive ABA triblock copolymer and its self-assembly into gels and micelles upon changes in pH.



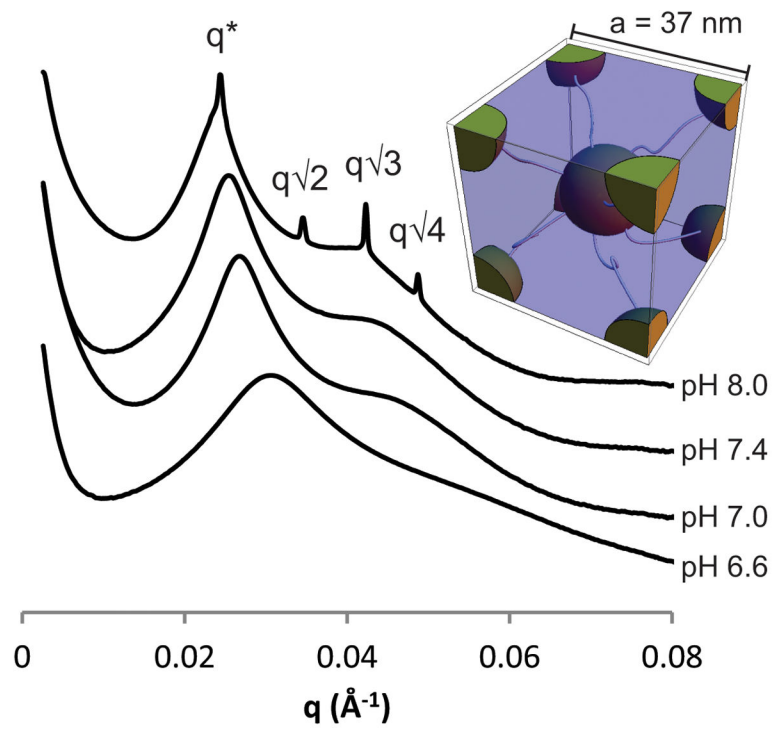
**Fig. 2.**  
 $^1\text{H-NMR}$  of **Hist-SH** (bottom), **PAGE<sub>3.5k</sub>-b-PEO<sub>20k</sub>-b-PAGE<sub>3.5k</sub>** (middle), and **PHGE-*b*-PEO-*b*-PHGE** (top).



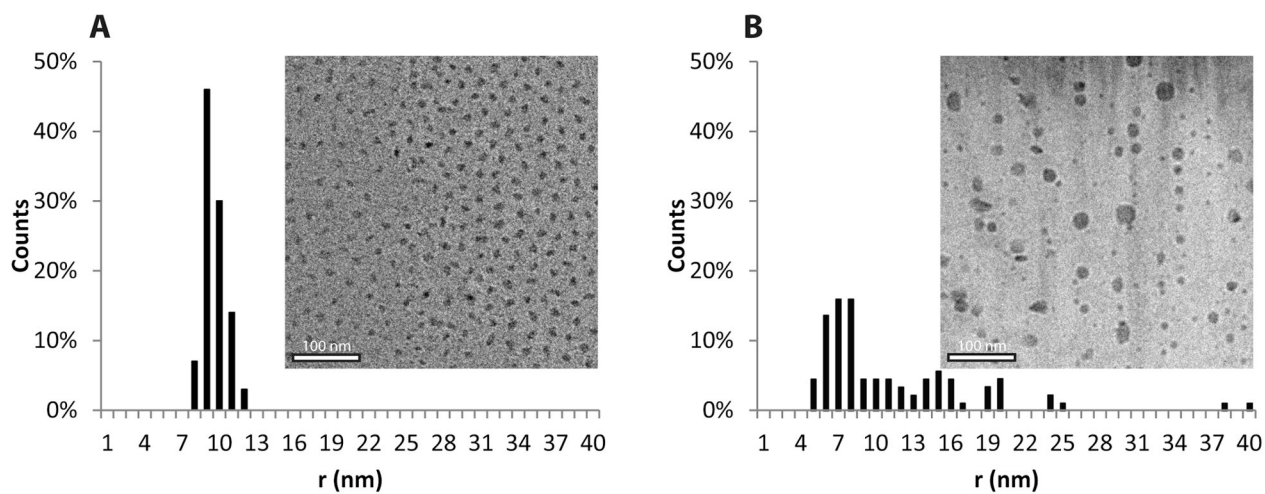
**Fig. 3.**  
Photo of 10 wt% gels/solutions of PHGE-*b*-PEO-*b*-PHGE at different pH.



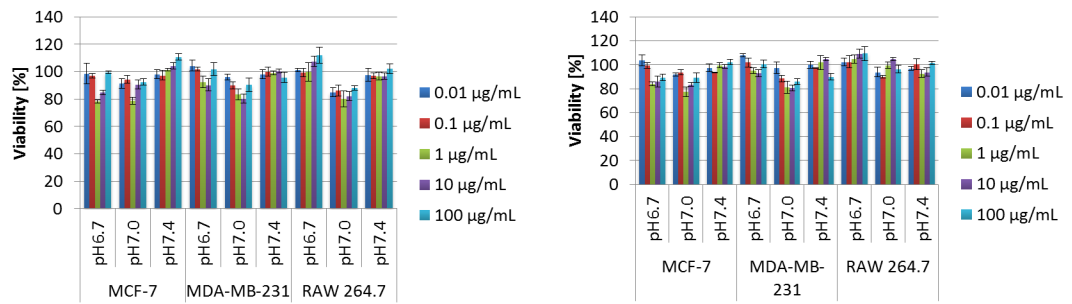
**Fig. 4.** Storage modulus ( $G'$ ) at 1 Hz vs. pH.  $G'$  values extracted from Figure ESI4.



**Fig. 5.** SAXS measurements of 10 wt% gels/solutions of **PHGE-*b*-PEO-*b*-PHGE** at different pH with inset of BCC unit cell.

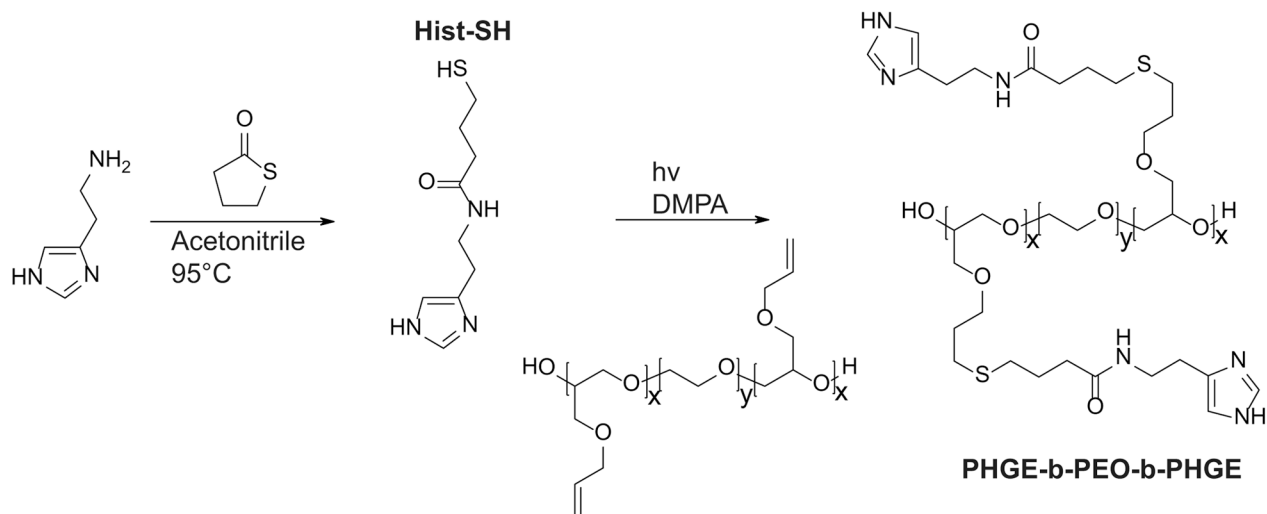


**Fig. 6.** Cryo-TEM image of a micelle solution at pH 7.4 and a histogram showing the distribution of particle sizes (A). Cryo-TEM image of a micelle solution at pH 5.0 and a histogram showing the distribution of particle sizes (B).



**Fig. 7.** MTT-assay of **PHGE-*b*-PEO-*b*-PHGE** after 48 h (left) and 72 h (right) using three different cell lines varying the concentration of polymer and pH.





**Scheme 1.**  
Synthetic route to **Hist-SH** and **PHGE-*b*-PEO-*b*-PHGE**.